THE JOURNAL OF PHYSICAL CHEMISTRY C
A JOURNAL OF THE AMERICAN CHEMICAL SOCIETY

pubs.acs.org/JPCC

Article

Enhanced Solar CO_2 Reduction Using Single Cobalt Sites on Carbon Nitride Modified with a Dianhydride

Published as part of The Journal of Physical Chemistry C special issue "Vicki H. Grassian Festschrift".

Allison St. John, Shuting Xiang, Hannah Flayhart, Eduardo Ortega, Qian Qian, N. Aaron Deskins, Beatriz Roldan Cuenya, Jonathan Rochford, Anatoly I. Frenkel,* and Gonghu Li*

Cite This: J. Phys. Chem. C 2025, 129, 7327−7334

Read Online

ACCESS | Metrics & More | Article Recommendations | Supporting Information

ABSTRACT: Photoactive single-atom catalysts (SACs) are among the most exciting catalytic materials for solar fuel production. Different SACs, including our own Co SACs, have been prepared on graphitic carbon nitride (C_3N_4) for use in photocatalysis. Building on our prior success, we report here doped C_3N_4 using various supplemental carbon dopants as the support for Co SACs. The Co SAC on a dianhydride-doped C_3N_4 showed the highest activity in photocatalytic CO_2 reduction. Catalyst characterization was carried out to explore the origin of the enhanced activity of this particular Co SAC. The dianhydride-doped C_3N_4 possesses unique microstructural features, including a large interlayer space and fibrous morphology, that could contribute to enhanced photocatalytic activity. Our results further indicate that dianhydride is the most effective dopant to incorporate aromatic moieties in C_3N_4, which resulted in improved charge separation and enhanced activity in photocatalysis.

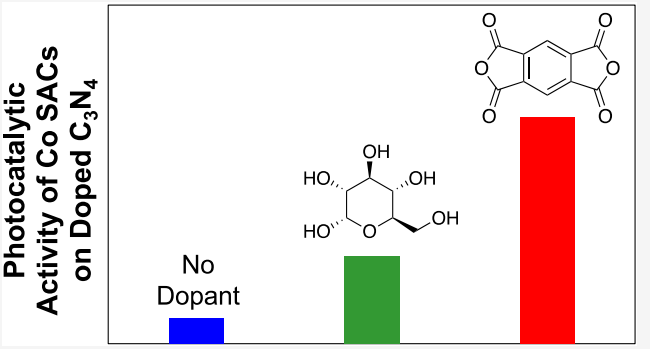

INTRODUCTION

In recent years, "single-atom" catalysts (SACs), which are atomically dispersed individual metal ions stabilized on a support, have attracted enormous interest for various chemical transformations due to their unique electronic structures and advantages over nanoparticles and other bulk metal counterparts.[1−4] Choosing appropriate supports for SACs in photocatalysis requires consideration of the binding ability of the metal atoms, the stability of such binding, and the resulting activity based on electronic structures and light absorption. Graphitic carbon nitride (C_3N_4) has been extensively explored as a metal-free photoactive material due to its low cost and narrow band gap.[5−8] On its own, C_3N_4 has relatively low activity in photocatalysis largely due to poor charge separation and lack of surface sites for selective catalysis. Instead, C_3N_4 has been employed as an excellent support for SACs as its nitrogen-rich structure enables the coordination of metals.[9−11] SACs containing atomically dispersed Fe, Co, Ni, Cu, Ag, Au, Ru, and even rare-earth-metal sites have been prepared on C_3N_4 for use in photocatalytic CO_2 reduction.[12−25]

Many recent papers investigated SACs based on Co, a nonprecious metal, on C_3N_4[26−36] and other supports[37−43] in different chemical transformations. Structural motifs of Co SACs on C_3N_4 have been discussed in previous work. Existing models for SACs in C_3N_4 include in-plane $M−N_3$ and interlayer $M−N_4$ coordination,[44] $C−M−N_2$ coordination,[12] $M−N_4$ coordination in the presence of N vacancies,[45] and other possible structures.[46−48] Unlike N-doped carbon materials featuring the cyclam-type coordination sphere, C_3N_4 contains "pockets" that allow only in-plane $M−N_2$ coordination with a reasonable M−N bond length. Our recent studies revealed a possible structure model of our Co SACs in C_3N_4 containing the $M−N_{2+2}$ moiety, where a metal center is coordinated with four N atoms at the edge sites of two C_3N_4 flakes.[31] Similar $M−N_{2+2}$ coordination SACs in graphene-based materials have been reported by others.[49−51]

In our recent work,[26,29,31] Co SACs were synthesized by depositing Co^{2+} on C_3N_4 via a microwave method. The resulting Co SACs produced CO as the major product in the photocatalytic CO_2 reduction. Photocatalytic activities of the Co SACs decreased drastically as the cobalt loading increased. Characterization of the Co SACs with X-ray absorption spectroscopy (XAS), including the X-ray absorption near-edge

Received: January 3, 2025
Revised: February 28, 2025
Accepted: March 24, 2025
Published: April 4, 2025

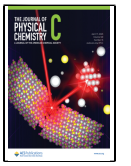

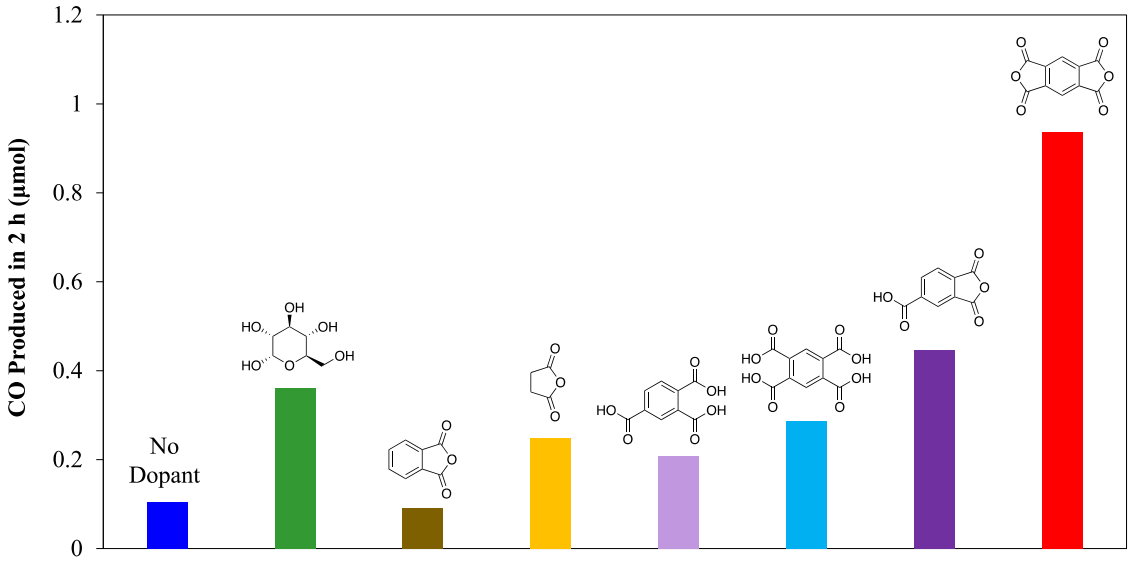

Figure 1. CO produced in the photocatalytic CO_2 reduction using 5 mg of Co SACs on C_3N_4 prepared in the absence (no dopant) and presence of different dopants (left to right: dextrose, phthalic anhydride, succinic anhydride, 1,2,4-benzenetricarboxylic acid, 1,2,4,5-benzenetetracarboxylic acid, 1,2,4-benzenetricarboxylic anhydride, and 1,2,4,5-benzenetetracarboxylic dianhydride). The Co SACs were prepared using 1 mg of $CoCl_2$ and 100 mg of C_3N_4. Loadings of Co in the samples were determined to be (from left to right) 0.043, 0.046, 0.036, 0.079, 0.058, 0.056, 0.050, and 0.064 μmol per mg of powder sample, respectively.

structure (XANES) and extended X-ray absorption fine structure (EXAFS), provided important information regarding the structure of the active sites. At low cobalt loadings, the presence of single Co^{2+} sites was confirmed by using XANES and EXAFS. At relatively high cobalt loadings, a significant portion of cobalt exists in the form of inactive cobalt oxides.

Supplemental carbon dopants have been used in the synthesis of C_3N_4 to improve its photocatalytic activity. It has been reported that the doping of C_3N_4 with carbon can improve its visible light absorption and inhibit charge recombination.[52] In our studies, doping C_3N_4 with carbon was found to be essential for the photocatalytic activities of Co SACs.[29] Carbon doping of C_3N_4 was achieved using small amounts of dextrose during the synthesis of C_3N_4 via the pyrolysis of urea. Building on our recent achievements, other supplemental carbon sources are being evaluated for their ability to enhance the photocatalytic activities of Co SACs on C_3N_4 by improving charge separation and optimizing the local coordination environment of Co^{2+} sites.

In this current work, we aim to design doped C_3N_4 containing nitrogen atoms in the framework that are in an ideal position for binding to the cobalt centers rather than relying on nitrogen atoms at edge sites. Modified C_3N_4 using different supplemental carbon dopants, including 1,2,4,5-benzenetetracarboxylic dianhydride, have been synthesized in order to enhance photoinduced charge separation and potentially build well-defined nitrogen binding sites into the polymeric structure of C_3N_4. The synthesized doped C_3N_4 and Co SACs are characterized with a variety of techniques and tested in photocatalytic CO_2 reduction. Through such experimental work, we attempt to correlate the photocatalytic activities of the synthesized Co SACs with the charge separation properties of the doped C_3N_4 and the local coordination environment of the Co^{2+} sites.

EXPERIMENTAL SECTION

Materials. Acetonitrile (ACN, 99.9%), methanol (99.8%), and chloroform (99.8%) were obtained from Fisher Chemical. Cobalt(II) chloride (>98%) was obtained from Sigma-Aldrich. Triethylamine (TEA, 99%), 1,2,4-benzenetricarboxylic acid (98%), and 1,2,4-benzene-tricarboxylic anhydride (97%) were obtained from Acros Organics. Urea (>99.5%), dextrose (anhydrous, 99.8%), phthalic anhydride (99%), succinic anhydride (99%), and 1,2,4,5-benzenetetracarboxylic acid (96%) were obtained from Thermo Fisher Scientific. 1,2,4,5-Benzenetetracarboxylic dianhydride (>98.0%) was purchased from TCI. Triethanolamine (TEOA, 99.0%) was purchased from Spectrum Chemical MFG Corp. All reagents were used without further purification.

Catalyst Synthesis. Modified carbon nitride materials were synthesized by the pyrolysis of urea in the presence of different dopants. In a typical synthesis, 20 g of urea was placed in a ceramic crucible with 20 mg of the dopant and ground until well mixed. The crucible was covered with aluminum foil and calcined in a muffle furnace for 4 h at 600 °C with a ramp rate of 5 °C/min. Pristine C_3N_4 was synthesized in the same way in the absence of any dopant. The resulting doped C_3N_4 was loaded with Co^{2+} via a microwave method. In particular, 100 mg of C_3N_4 was mixed with a certain amount (0.25−10 mg) of $CoCl_2$ in 7.5 mL of acetonitrile in a capped reaction vessel. The suspension was placed in a sonicator bath for 5 min, followed by 30 min of stirring. Then, 65 μL of TEA was added, followed by an additional 30 min of stirring. The suspension was placed in a CEM Discover single-mode microwave reactor and was heated to 80 °C for 2 h. The resulting material was recovered by centrifugation and washed twice with chloroform, methanol, and acetonitrile. The final material was left to dry at room temperature. The C_3N_4 materials synthesized in the presence of dextrose and 1,2,4,5-benzenetetracarboxylic dianhydride are denoted as "C-C_3N_4" and "DA-C_3N_4", respectively.

https://doi.org/10.1021/acs.jpcc.4c08562
J. Phys. Chem. C 2025, 129, 7327−7334

Material Characterization. UV−visible spectra were obtained on a Cary 50 Bio spectrophotometer with a Barrelino diffuse reflectance attachment using $BaSO_4$ as a background. Photoluminescence spectra were obtained on a Cary Eclipse fluorimeter with a solid sample holder, where emission spectra were recorded at a 355 nm excitation wavelength. Powder X-ray diffraction (XRD) patterns were obtained on a LabX XRD-6100 diffractometer using a Cu Kα source (λ = 0.154 nm). Scanning electron microscopy (SEM) images were taken on a Lyra3 GMU FIB SEM. Transmission electron microscopy (TEM) images and energy-dispersive X-ray spectroscopy (EDS) were acquired using a Talos F200X (Thermo Fisher Scientific) STEM operated at 200 kV and an electron probe of 72 pA and a 10.5 mrad convergence semiangle. The EDS quantification was performed using Velox software v1.4.2 (Thermo Fisher Scientific). Elemental analysis was conducted by acid extraction of the cobalt-loaded-doped C_3N_4 materials and subsequent cobalt quantization on an Agilent 4210 microwave plasma atomic emission spectroscopy (MP-AES). Diffuse reflectance infrared Fourier transform spectra (DRIFTS) were obtained using a Harrick Praying Mantis diffuse reflectance IR cell attached to a Thermo Nicolet 6700 FT-IR spectrometer.

X-ray Absorption Spectroscopy (XAS). X-ray absorption spectra at the Co K-edge were taken at the 7-BM QAS beamline of NSLS-II at Brookhaven National Laboratory. Si(111) double crystal was used as a monochromator. 15 cm long ion chambers, filled with 100% N_2, were used for the detection of incident and transmitted beams, and a passivated implanted planar silicon detector with a Fe filter (with the thickness corresponding to 6 absorption lengths at Co K-edge energy) was used for the detection of fluorescence. Measurements were performed in an ambient atmosphere at room temperature. Cobalt on DA-C_3N_4, C-C_3N_4, and C_3N_4 at all loadings and conditions was measured in the fluorescence mode. Cobalt on other doped C_3N_4 was measured in transmission mode.

Photocatalytic Testing. In the photocatalytic CO_2 reduction, 1 mg of a synthesized catalyst was dispersed in 4 mL of a mixture of acetonitrile (ACN) and triethanolamine (TEOA) (ACN/TEOA = 4:1 (v/v)) in a quartz test tube. The sealed test tube was bubbled with CO_2 in the dark with stirring for 20 min. The vessel was then irradiated with a halogen lamp with a water filter at an intensity of 200 mW/cm^2. Each 30 min, the headspace was sampled and analyzed using an Agilent 7820 GC with a TCD detector and a 60/80 Carboxen-1000 packed column. Initial screening results (Figure 1) were obtained using 5 mg of the catalyst.

RESULTS AND DISCUSSION

Several doped C_3N_4 materials have been synthesized via the pyrolysis of urea at 600 °C in the presence of supplemental carbon dopants, including dextrose, phthalic anhydride, succinic anhydride, 1,2,4-benzenetricarboxylic acid, 1,2,4,5-benzenetetracarboxylic acid, 1,2,4-benzenetricarboxylic anhydride, and 1,2,4,5-benzenetetracarboxylic dianhydride. Following our established procedure,[31] Co SACs were prepared by depositing Co^{2+} on the synthesized C_3N_4 materials. The synthesized C_3N_4 materials and Co SACs were characterized by a variety of techniques, including UV−vis, XRD, SEM, XAS, DRIFTS, and photoluminescence spectroscopy. In the photocatalytic CO_2 reduction, a Co SAC on C_3N_4 prepared in the presence of 1,2,4,5-benzenetetracarboxylic dianhydride, denoted "Co^{2+}@DA-C_3N_4", showed the highest activity among all of the synthesized Co SACs (Figure 1).

While it is unclear how these supplemental carbon dopants modified the C_3N_4 structure at the molecular level, it is evident that 1,2,4,5-benzenetetracarboxylic dianhydride is the most efficient dopant to incorporate aromatic moieties in C_3N_4 and introduce other structural changes, as will be discussed further. Three Co SACs, Co^{2+}@DA-C_3N_4, Co^{2+}@C-C_3N_4 (Co SAC on C-C_3N_4), and Co^{2+}@C_3N_4 (Co SAC on pristine C_3N_4), are selected for further investigation in order to explore structural characteristics responsible for enhanced activity in photocatalysis. Figure 2 describes the relative activity of these three

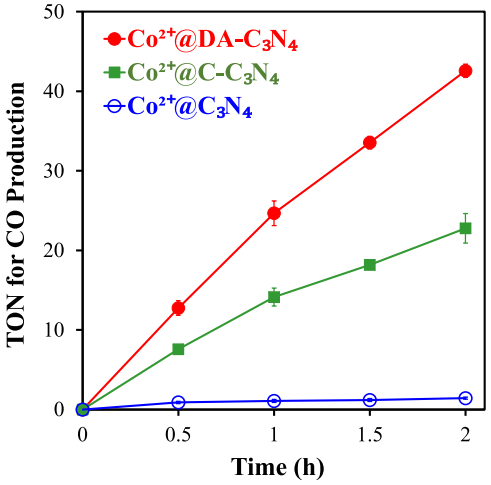

Figure 2. CO production during the photocatalytic CO_2 reduction under light irradiation with a light intensity of 200 mW cm^{-2}. Error bars were obtained from triplicate data points using three different samples measured under the same conditions. The Co SACs were prepared using 0.25 mg of $CoCl_2$ and 100 mg of C_3N_4. Loadings of Co were determined to be 0.022, 0.019, and 0.019 μmol per mg of C_3N_4, C-C_3N_4, and DA-C_3N_4, respectively.

selected Co SACs in the photocatalytic CO_2 reduction. Under the experimental conditions employed in this study, Co^{2+}@C_3N_4 showed negligible activity, while turnover numbers (TONs) for CO production of 43 and 23 were obtained after photocatalysis for 2 h using Co^{2+}@DA-C_3N_4 and Co^{2+}@C-C_3N_4, respectively. In order to confirm the source of CO produced in photocatalysis, isotope labeling studies were conducted using $^{13}CO_2$ instead of the regular $^{12}CO_2$.[53,54] Under experimental conditions employed in this study, only ^{13}CO was detected in the photocatalytic $^{13}CO_2$ reduction, as can be seen from the infrared spectrum of the headspace gases above the reaction solution (see Figure S1).

The synthesized Co SACs were characterized by X-ray absorption spectroscopy (XAS), including an X-ray absorption near-edge structure (XANES) and extended X-ray absorption fine structure (EXAFS). At relatively low loadings of cobalt, XANES and EXAFS data of Co^{2+}@DA-C_3N_4 clearly show single-site characteristics.[55−57] For instance, its XANES spectral shape is different from those of CoO and Co_3O_4 (Figure 3), likely due to the coordination of isolated Co^{2+} with the N atoms in DA-C_3N_4. In its EXAFS spectrum shown in Figure 4, a peak around 1.55 Å (uncorrected for the photoelectron phase shift) is present, and no Co−O−Co contribution can be detected, indicating the coordination of Co^{2+} with N atoms. Therefore, cobalt species in this sample

https://doi.org/10.1021/acs.jpcc.4c08562
J. Phys. Chem. C 2025, 129, 7327−7334

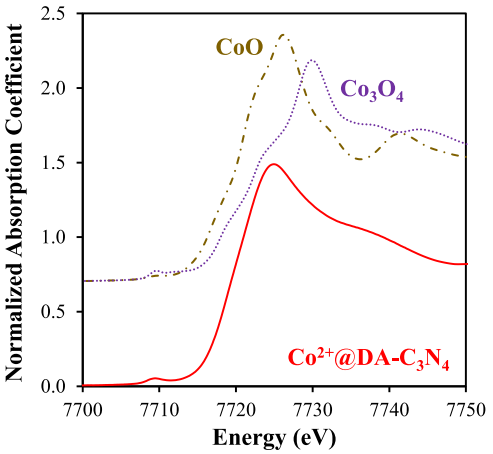

Figure 3. Normalized Co K-edge XANES spectra of Co^{2+}@DA-C_3N_4 (cobalt loading 0.019 μmol/mg), and CoO and Co_3O_4 as references.

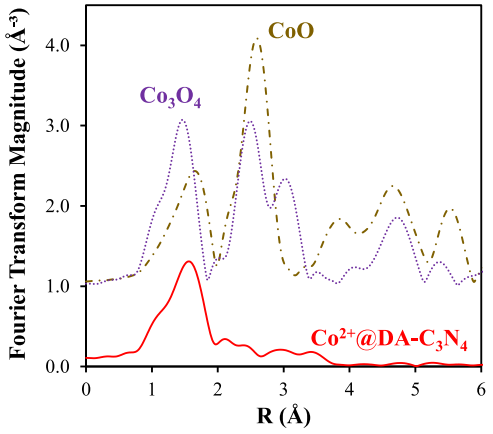

Figure 4. Fourier transform magnitudes of k^2-weighted Co K-edge EXAFS spectra of Co^{2+}@DA-C_3N_4 (cobalt loading 0.019 μmol/mg), and CoO and Co_3O_4 as references.

exist as single Co^{2+} sites. In comparison, a peak at around 2.7 Å corresponding to the Co−O−Co bond in the CoO structure is present in the EXAFS spectrum of Co^{2+}@DA-C_3N_4 at a relatively high cobalt loading (Figure S2). Electron microscopy studies further confirmed the presence of CoO nanoparticles in Co^{2+}@DA-C_3N_4 at this high cobalt loading (Figure S3). Similar to our previous observation,[26] such CoO nanoparticles are inactive in the photocatalytic CO_2 reduction since Co^{2+}@DA-C_3N_4 at relatively high loadings, when NPs are more likely formed, are much less active than those at lower cobalt loadings (Figure S4). Additional EXAFS results (Figure S5) indicate that Co SACs in Co^{2+}@DA-C_3N_4 remained atomically dispersed after photocatalysis under the experimental conditions employed in this study.

The EXAFS spectra shown in Figure 4 were further analyzed to extract structural information including the coordination geometry of the Co SACs. The fitting results indicate a negligible difference among the coordination geometry of Co^{2+}@C_3N_4, Co^{2+}@C-C_3N_4, and Co^{2+}@DA-C_3N_4 (Figures S6 and S7 and Table S1). For example, the coordination numbers of the Co center were ∼ 6 for the three Co SACs, while the average Co−N/Co−O bond lengths were between 2.05 and 2.07 Å.

The synthesized C_3N_4 materials were characterized by additional techniques in order to help understand the comparison shown in Figure 2. In particular, powder X-ray diffraction (XRD) patterns of DA-C_3N_4, C-C_3N_4, and pristine C_3N_4 were collected to provide information regarding their crystal structure. A prominent peak at around 2θ = 27.7° is seen in the XRD patterns of the three samples (Figure 5).

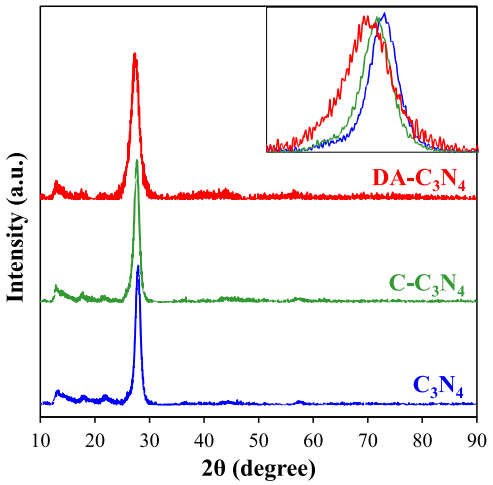

Figure 5. Powder X-ray diffraction patterns of C_3N_4, C-C_3N_4, and DA-C_3N_4. Inset: close-up view of the diffraction patterns in the range of 28−30°.

Close examination indicates that this peak for DA-C_3N_4 is broader and is shifted to a smaller 2θ value, compared to those for C-C_3N_4 and C_3N_4 (Figure 5, inset). Such a comparison suggests that the dopant for DA-C_3N_4 (1,2,4,5-benzenetetracarboxylic dianhydride) caused more significant disruption to the C_3N_4 framework structure than the dopant for C-C_3N_4 (dextrose). Furthermore, the observed peak shift indicates a slightly larger interlayer space for DA-C_3N_4 relative to C-C_3N_4 and DA-C_3N_4.

Scanning electron microscopy (SEM) images were collected to compare the morphology of the three samples. While C_3N_4 and C-C_3N_4 have similar morphology, DA-C_3N_4 appears to have a more fibrous structure (Figure 6). This comparison in morphology suggests that using the dianhydride dopant may lead to more controlled self-assembly during polymerization. Subsequently, DA-C_3N_4 has a slightly higher surface area (101.2 m^2/g) than C-C_3N_4 (94.7 m^2/g) and pristine C_3N_4 (86.4 m^2/g).

The results shown in Figures 5 and 6 indicate that DA-C_3N_4 has a different microstructure than C-C_3N_4 and pristine C_3N_4, although the infrared spectra of the three samples are almost identical (Figure S8). Such a difference could partially contribute to the relatively higher activity of Co^{2+}@DA-C_3N_4 than Co^{2+}@C_3N_4 and Co^{2+}@C-C_3N_4 (Figure 2). We also examined the light absorption ability of these materials. Pristine C_3N_4 has a band gap of around 2.7 eV and can harvest photons with a wavelength of up to 460 nm.[5,58] It has been shown that appropriate carbon doping can improve its photoresponse in the visible region (400−800 nm).[29,59] In our study, both DA-C_3N_4 and C-C_3N_4 have significant photoresponse in the visible region, compared to pristine C_3N_4 (Figure 7). However, DA-C_3N_4 and C-C_3N_4 share similar absorption features in the visible region. It is unlikely that their light absorption ability contributed significantly to the observed difference in the photocatalytic activity, as shown in Figure 2. A similar photoresponse in the visible region was

https://doi.org/10.1021/acs.jpcc.4c08562
J. Phys. Chem. C 2025, 129, 7327−7334

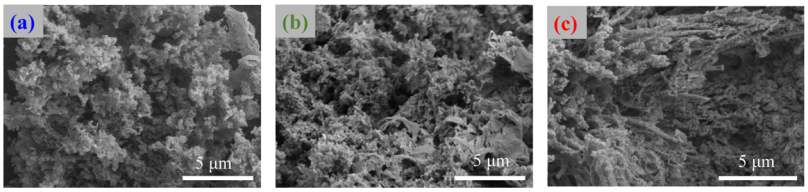

Figure 6. SEM images of (a) pristine C_3N_4, (b) C-C_3N_4, and (c) DA-C_3N_4.

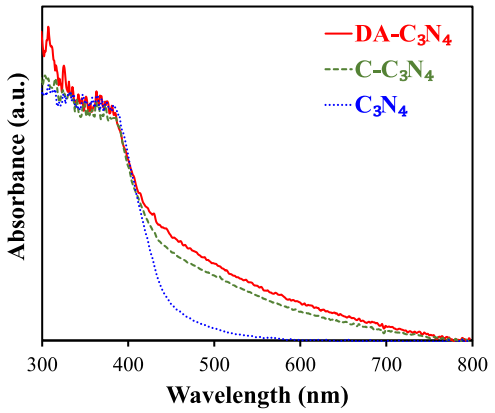

Figure 7. Diffuse reflectance UV−vis spectra of C_3N_4, C-C_3N_4, and DA-C_3N_4.

also observed in the spectra of other doped C_3N_4 samples (Figures S9 and S10), except for the one doped with phthalic anhydride (Figure S9a).

Incorporation of aromatic moieties into the C_3N_4 matrix has been reported to result in extended π-conjugation, which alters the optical absorption and improves charge separation.[60−62] We characterized the photophysical properties of the synthesized C_3N_4 samples with photoluminescence spectroscopy. In the spectrum of pristine C_3N_4, an intense and broad emission band in the range between 400 and 600 nm is present, indicating significant charge recombination from the photoexcited state (Figure 8). This band is much less intense in the spectra of DA-C_3N_4 and C-C_3N_4. Furthermore, the emission features in the spectrum of DA-C_3N_4 are less intense than those of C-C_3N_4. It has been reported that C doping

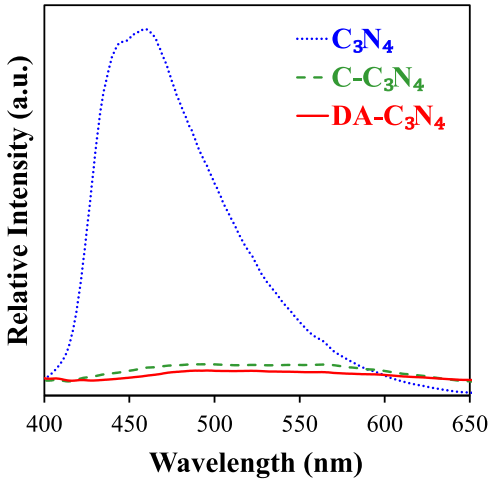

Figure 8. Photoluminescence spectra of C_3N_4, C-C_3N_4, and DA-C_3N_4.

improves photoinduced charge separation in C_3N_4.[63−67] In this study, the addition of Co SACs to the C_3N_4 samples led to negligible changes in their emission spectra (Figure S11). The comparison in the photocatalytic activity shown in Figure 2 correlates well with charge separation, as inferred from the quenching of the emission band shown in Figure 8. Therefore, the higher photocatalytic activity of Co^{2+}@DA-C_3N_4 compared to that of Co^{2+}@C-C_3N_4 is at least partly due to the improved charge separation of the former.

It should be noted that several of the synthesized doped C_3N_4 materials, in particular, those doped with succinic anhydride, 1,2,4-benzenetricarboxylic acid and 1,2,4,5-benzenetetracarboxylic acid, demonstrated enhanced charge separation as evidenced by the low intensity of their emission spectra (Figure S12). However, Co SACs on these doped C_3N_4 materials were shown to be less active than Co^{2+}@C-C_3N_4 in photocatalysis (Figure 1). We are mindful that comparing the photoluminescence intensity only provides indirect information regarding the efficiency of photoinduced charge separation in the C_3N_4 materials. Additional experimental analysis, such as time-resolved spectroscopic studies, would be more convincing in evaluating the charge separation efficiency. We are currently working toward this goal and hope to report such results in a future communication.

One drawback of the synthesized Co SACs is their stability under photochemical conditions. In our study, elemental analysis was conducted to evaluate the robustness of Co SACs. Partial loss of the coordinated Co^{2+} ions was observed for the Co SACs. According to our elemental analysis results, 44, 51, and 66% of Co^{2+} ions remained coordinated to C_3N_4, C-C_3N_4, and DA-C_3N_4, respectively, after photocatalysis for 2 h using the corresponding Co SACs. Subsequently, the Co SACs appeared to be less active after repeated use in photocatalysis, likely due to the loss of coordinated Co^{2+} ions (Figure S13).

CONCLUSIONS

In summary, we have synthesized a variety of doped C_3N_4 as a support for Co SACs. The Co SAC on a dianhydride-doped C_3N_4 showed the highest activity in the photocatalytic CO_2 reduction. Selected C_3N_4 and SACs are characterized by different techniques to explore the origin of the observed enhancement in photocatalytic activity. The dianhydride-doped C_3N_4 possesses unique microstructural features, including a large interlayer space and fibrous morphology, that could contribute to enhanced photocatalytic activity. Improved charge separation, inferred from photoluminescence spectroscopy, was also observed using the dianhydride-doped C_3N_4. Our work contributes to the development of innovative photocatalytic materials by correlating the synthesis of SACs as photocatalysts with their structural and functional properties.

https://doi.org/10.1021/acs.jpcc.4c08562
J. Phys. Chem. C 2025, 129, 7327−7334

■ ASSOCIATED CONTENT

Supporting Information

The Supporting Information is available free of charge at https://pubs.acs.org/doi/10.1021/acs.jpcc.4c08562.

Additional infrared, UV−vis, photoluminescence, and EXAFS spectra; photocatalysis results; TEM images; and EXAFS analysis results (PDF)

■ AUTHOR INFORMATION

Corresponding Authors

Anatoly I. Frenkel − *Department of Materials Science and Chemical Engineering, Stony Brook University, Stony Brook, New York 11794, United States; Division of Chemistry, Brookhaven National Laboratory, Upton, New York 11973, United States;* orcid.org/0000-0002-5451-1207; Email: anatoly.frenkel@stonybrook.edu

Gonghu Li − *Department of Chemistry, University of New Hampshire, Durham, New Hampshire 03857, United States;* orcid.org/0000-0002-2924-3597; Email: gonghu.li@unh.edu

Authors

Allison St. John − *Department of Chemistry, University of New Hampshire, Durham, New Hampshire 03857, United States*

Shuting Xiang − *Department of Materials Science and Chemical Engineering, Stony Brook University, Stony Brook, New York 11794, United States*

Hannah Flayhart − *Department of Chemistry, University of Massachusetts Boston, Boston, Massachusetts 02125, United States*

Eduardo Ortega − *Department of Interface Science, Fritz Haber Institute of the Max Planck Society, Berlin 14195, Germany;* orcid.org/0000-0002-0643-5190

Qian Qian − *Department of Chemical Engineering, Worcester Polytechnic Institute, Worcester, Massachusetts 01609, United States*

N. Aaron Deskins − *Department of Chemical Engineering, Worcester Polytechnic Institute, Worcester, Massachusetts 01609, United States;* orcid.org/0000-0002-0041-7960

Beatriz Roldan Cuenya − *Department of Interface Science, Fritz Haber Institute of the Max Planck Society, Berlin 14195, Germany;* orcid.org/0000-0002-8025-307X

Jonathan Rochford − *Department of Chemistry, University of Massachusetts Boston, Boston, Massachusetts 02125, United States;* orcid.org/0000-0003-2397-9162

Complete contact information is available at: https://pubs.acs.org/10.1021/acs.jpcc.4c08562

Notes

The authors declare no competing financial interest.

■ ACKNOWLEDGMENTS

This material was based upon work supported by the US National Science Foundation under Awards 2102655 to G.L., 2102299 to A.I.F., and 2102198 to N.A.D. This research used beamline 7-BM (QAS) of the National Synchrotron Light Source II, a US DOE Office of Science User Facility operated for the DOE Office of Science by Brookhaven National Laboratory under Contract No. DE-SC0012704. Beamline operations were supported in part by the Synchrotron Catalysis Consortium (US DOE, Office of Basic Energy Sciences, Grant No. DE-SC0012335). The authors thank Dr. Lu Ma for her help with XAS measurements at the QAS beamline. SEM images and XRD were collected on facilities at the UNH University Instrumentation Center.

■ REFERENCES

(1) Wang, A.; Li, J.; Zhang, T. Heterogeneous single-atom catalysis. *Nat. Rev. Chem.* **2018**, *2* (6), 65−81.

(2) Cui, X.; Li, W.; Ryabchuk, P.; Junge, K.; Beller, M. Bridging homogeneous and heterogeneous catalysis by heterogeneous single-metal-site catalysts. *Nat. Catal.* **2018**, *1* (6), 385−397.

(3) Gao, C.; Low, J.; Long, R.; Kong, T.; Zhu, J.; Xiong, Y. Heterogeneous Single-Atom Photocatalysts: Fundamentals and Applications. *Chem. Rev.* **2020**, *120* (21), 12175−12216.

(4) Liu, L.; Li, M.; Chen, F.; Huang, H. Recent Advances on Single-Atom Catalysts for CO_2 Reduction. *Small Struct.* **2023**, *4* (3), No. 2200188.

(5) Cao, S.; Low, J.; Yu, J.; Jaroniec, M. Polymeric Photocatalysts Based on Graphitic Carbon Nitride. *Adv. Mater.* **2015**, *27* (13), 2150−2176.

(6) Xia, T.; Long, R.; Gao, C.; Xiong, Y. Design of atomically dispersed catalytic sites for photocatalytic CO_2 reduction. *Nanoscale* **2019**, *11* (23), 11064−11070.

(7) Li, Y.; Kong, T.; Shen, S. Artificial Photosynthesis with Polymeric Carbon Nitride: When Meeting Metal Nanoparticles, Single Atoms, and Molecular Complexes. *Small* **2019**, *15* (32), No. 1900772.

(8) Zhao, M.; Feng, J.; Yang, W.; Song, S.; Zhang, H. Recent Advances in Graphitic Carbon Nitride Supported Single-Atom Catalysts for Energy Conversion. *ChemCatChem* **2021**, *13* (5), 1250−1270.

(9) Wang, Y.; Mao, J.; Meng, X.; Yu, L.; Deng, D.; Bao, X. Catalysis with Two-Dimensional Materials Confining Single Atoms: Concept, Design, and Applications. *Chem. Rev.* **2019**, *119* (3), 1806−1854.

(10) Fu, J.; Liu, K.; Jiang, K.; Li, H.; An, P.; Li, W.; Zhang, N.; Li, H.; Xu, X.; Zhou, H.; et al. Graphitic Carbon Nitride with Dopant Induced Charge Localization for Enhanced Photoreduction of CO_2 to CH_4. *Adv. Sci.* **2019**, *6* (18), No. 1900796.

(11) Kaiser, S. K.; Chen, Z.; Faust Akl, D.; Mitchell, S.; Pérez-Ramírez, J. Single-Atom Catalysts across the Periodic Table. *Chem. Rev.* **2020**, *120* (21), 11703−11809.

(12) Wang, J.; Heil, T.; Zhu, B.; Tung, C.-W.; Yu, J.; Chen, H. M.; Antonietti, M.; Cao, S. A Single Cu-Center Containing Enzyme-Mimic Enabling Full Photosynthesis under CO_2 Reduction. *ACS Nano* **2020**, *14* (7), 8584−8593.

(13) Yang, Y.; Li, F.; Chen, J.; Fan, J.; Xiang, Q. Single Au Atoms Anchored on Amino-Group-Enriched Graphitic Carbon Nitride for Photocatalytic CO_2 Reduction. *ChemSusChem* **2020**, *13* (8), 1979−1985.

(14) Cheng, L.; Yin, H.; Cai, C.; Fan, J.; Xiang, Q. Single Ni As Few-Layer g-C_3N_4 for Photocatalytic CO_2 Reduction: The Role of Edge Confinement. *Small* **2020**, *16* (28), No. 2002411.

(15) Li, Y.; Li, B.; Zhang, D.; Cheng, L.; Xiang, Q. Crystalline Carbon Nitride Supported Copper Single Atoms for Photocatalytic CO_2 Reduction with Nearly 100% CO Selectivity. *ACS Nano* **2020**, *14* (8), 10552−10561.

(16) Chen, P.; Lei, B.; Dong, Xa.; Wang, H.; Sheng, J.; Cui, W.; Li, J.; Sun, Y.; Wang, Z.; Dong, F. Rare-Earth Single-Atom La−N Charge-Transfer Bridge on Carbon Nitride for Highly Efficient and Selective Photocatalytic CO_2 Reduction. *ACS Nano* **2020**, *14* (11), 15841−15852.

(17) Ji, S.; Qu, Y.; Wang, T.; Chen, Y.; Wang, G.; Li, X.; Dong, J.; Chen, Q.; Zhang, W.; Zhang, Z.; et al. Rare-Earth Single Erbium Atoms for Enhanced Photocatalytic CO_2 Reduction. *Angew. Chem., Int. Ed.* **2020**, *59* (26), 10651−10657.

(18) Zhao, Z.; Liu, W.; Shi, Y.; Zhang, H.; Song, X.; Shang, W.; Hao, C. An insight into the reaction mechanism of CO_2 photoreduction

catalyzed by atomically dispersed Fe atoms supported on graphitic carbon nitride. *Phys. Chem. Chem. Phys.* **2021**, *23* (8), 4690−4699.
(19) Zhang, J.-H.; Yang, W.; Zhang, M.; Wang, H.-J.; Si, R.; Zhong, D.-C.; Lu, T.-B. Metal-organic layers as a platform for developing single-atom catalysts for photochemical CO_2 reduction. *Nano Energy* **2021**, *80*, No. 105542.
(20) Cometto, C.; Ugolotti, A.; Grazietti, E.; Moretto, A.; Bottaro, G.; Armelao, L.; Di Valentin, C.; Calvillo, L.; Granozzi, G. Copper single-atoms embedded in 2D graphitic carbon nitride for the CO_2 reduction. *npj 2D Mater. Appl.* **2021**, *5* (1), 63.
(21) Sharma, P.; Kumar, S.; Tomanec, O.; Petr, M.; Zhu Chen, J.; Miller, J. T.; Varma, R. S.; Gawande, M. B.; Zbořil, R. Carbon Nitride-Based Ruthenium Single Atom Photocatalyst for CO_2 Reduction to Methanol. *Small* **2021**, *17* (16), No. 2006478.
(22) Wang, Y.; Qu, Y.; Qu, B.; Bai, L.; Liu, Y.; Yang, Z.-D.; Zhang, W.; Jing, L.; Fu, H. Construction of Six-Oxygen-Coordinated Single Ni Sites on g-C_3N_4 with Boron-Oxo Species for Photocatalytic Water-Activation-Induced CO_2 Reduction. *Adv. Mater.* **2021**, *33* (48), No. 2105482.
(23) Sun, X.; Sun, L.; Li, G.; Tuo, Y.; Ye, C.; Yang, J.; Low, J.; Yu, X.; Bitter, J. H.; Lei, Y.; et al. Phosphorus Tailors the d-Band Center of Copper Atomic Sites for Efficient CO_2 Photoreduction under Visible-Light Irradiation. *Angew. Chem., Int. Ed.* **2022**, *61* (38), No. e202207677.
(24) Ou, H.; Ning, S.; Zhu, P.; Chen, S.; Han, A.; Kang, Q.; Hu, Z.; Ye, J.; Wang, D.; Li, Y. Carbon Nitride Photocatalysts with Integrated Oxidation and Reduction Atomic Active Centers for Improved CO_2 Conversion. *Angew. Chem., Int. Ed.* **2022**, *61* (34), No. e202206579.
(25) Deng, A.; Zhao, E.; Li, Q.; Sun, Y.; Liu, Y.; Yang, S.; He, H.; Xu, Y.; Zhao, W.; Song, H.; et al. Atomic Cobalt−Silver Dual-Metal Sites Confined on Carbon Nitride with Synergistic Ag Nanoparticles for Enhanced CO_2 Photoreduction. *ACS Nano* **2023**, *17* (12), 11869−11881.
(26) Huang, P.; Huang, J.; Pantovich, S. A.; Carl, A. D.; Fenton, T. G.; Caputo, C. A.; Grimm, R. L.; Frenkel, A. I.; Li, G. Selective CO_2 Reduction Catalyzed by Single Cobalt Sites on Carbon Nitride under Visible-Light Irradiation. *J. Am. Chem. Soc.* **2018**, *140* (47), 16042−16047.
(27) Chu, C.; Zhu, Q.; Pan, Z.; Gupta, S.; Huang, D.; Du, Y.; Weon, S.; Wu, Y.; Muhich, C.; Stavitski, E.; et al. Spatially separating redox centers on 2D carbon nitride with cobalt single atom for photocatalytic H_2O_2 production. *Proc. Natl. Acad. Sci. U.S.A.* **2020**, *117* (12), 6376−6382.
(28) Wang, S.; Li, J.; Li, Q.; Bai, X.; Wang, J. Metal single-atom coordinated graphitic carbon nitride as an efficient catalyst for CO oxidation. *Nanoscale* **2020**, *12* (1), 364−371.
(29) Huang, P.; Huang, J.; Li, J.; Zhang, L.; He, J.; Caputo, C. A.; Frenkel, A. I.; Li, G. Effect of Carbon Doping on CO_2-Reduction Activity of Single Cobalt Sites in Graphitic Carbon Nitride. *ChemNanoMat* **2021**, *7* (9), 1051−1056.
(30) Xiong, Y.; Sun, W.; Han, Y.; Xin, P.; Zheng, X.; Yan, W.; Dong, J.; Zhang, J.; Wang, D.; Li, Y. Cobalt single atom site catalysts with ultrahigh metal loading for enhanced aerobic oxidation of ethylbenzene. *Nano Res.* **2021**, *14* (7), 2418−2423.
(31) Huang, P.; Huang, J.; Li, J.; Pham, T. D.; Zhang, L.; He, J.; Brudvig, G. W.; Deskins, N. A.; Frenkel, A. I.; Li, G. Revealing the Structure of Single Cobalt Sites in Carbon Nitride for Photocatalytic CO_2 Reduction. *J. Phys. Chem. C* **2022**, *126* (20), 8596−8604.
(32) Liu, X.; Deng, Y.; Zheng, L.; Kesama, M. R.; Tang, C.; Zhu, Y. Engineering Low-Coordination Single-Atom Cobalt on Graphitic Carbon Nitride Catalyst for Hydrogen Evolution. *ACS Catal.* **2022**, *12* (9), 5517−5526.
(33) Wang, Z.; Almatrafi, E.; Wang, H.; Qin, H.; Wang, W.; Du, L.; Chen, S.; Zeng, G.; Xu, P. Cobalt Single Atoms Anchored on Oxygen-Doped Tubular Carbon Nitride for Efficient Peroxymonosulfate Activation: Simultaneous Coordination Structure and Morphology Modulation. *Angew. Chem., Int. Ed.* **2022**, *61* (29), No. e202202338.
(34) Ding, J.; Teng, Z.; Su, X.; Kato, K.; Liu, Y.; Xiao, T.; Liu, W.; Liu, L.; Zhang, Q.; Ren, X.; et al. Asymmetrically coordinated cobalt single atom on carbon nitride for highly selective photocatalytic oxidation of CH_4 to CH_3OH. *Chem* **2023**, *9* (4), 1017−1035.
(35) Liu, X.; Huang, D.; Lai, C.; Qin, L.; Liu, S.; Zhang, M.; Fu, Y. Single cobalt atom anchored on carbon nitride with cobalt nitrogen/oxygen active sites for efficient Fenton-like catalysis. *J. Colloid Interface Sci.* **2023**, *629*, 417−427.
(36) Agrawal, S.; Casanova, D.; Trivedi, D. J.; Prezhdo, O. V. Enhanced Charge Separation in Single Atom Cobalt Based Graphitic Carbon Nitride: Time Domain Ab Initio Analysis. *J. Phys. Chem. Lett.* **2024**, *15* (8), 2202−2208.
(37) Di, J.; Chen, C.; Yang, S.-Z.; Chen, S.; Duan, M.; Xiong, J.; Zhu, C.; Long, R.; Hao, W.; Chi, Z.; et al. Isolated single atom cobalt in Bi_3O_4Br atomic layers to trigger efficient CO_2 photoreduction. *Nat. Commun.* **2019**, *10* (1), No. 2840.
(38) Xu, Q.; Jin, Y.; Sun, T.; Zheng, T.; Zhang, P.; Han, Y.; Wang, Y.; Li, T.; Qi, D.; Xu, L.; et al. Theoretical and experimental investigation of the coordination effect on photocatalytic CO_2 reduction efficiency of cobalt single atom catalyst. *Chem. Eng. J.* **2024**, *479*, No. 147837.
(39) Wang, Y.; Zheng, T.; Jin, Y.; Sun, T.; Ding, X.; Wang, X.; Xu, Q.; Li, T.; Zhang, S.; Jiang, J. Multiscale structural engineering of cobalt single-atom catalyst for highly efficient photocatalytic CO_2 reduction. *Sci. China Mater.* **2024**, *67* (4), 1292−1300.
(40) Wang, C.; Ren, H.; Wang, Z.; Guan, Q.; Liu, Y.; Li, W. A promising single-atom Co-N-C catalyst for efficient CO_2 electroreduction and high-current solar conversion of CO_2 to CO. *Appl. Catal., B* **2022**, *304*, No. 120958.
(41) Martini, A.; Timoshenko, J.; Ruscher, M.; Hursan, D.; Monteiro, M. C. O.; Liberra, E.; Roldan Cuenya, B. Revealing the structure of the active sites for the electrocatalytic CO_2 reduction to CO over Co single atom catalysts using operando XANES and machine learning. *J. Synchrotron Radiat.* **2024**, *31* (4), 741−750.
(42) Pei, J.; Shang, H.; Mao, J.; Chen, Z.; Sui, R.; Zhang, X.; Zhou, D.; Wang, Y.; Zhang, F.; Zhu, W.; et al. A replacement strategy for regulating local environment of single-atom Co-S_xN_{4-x} catalysts to facilitate CO_2 electroreduction. *Nat. Commun.* **2024**, *15* (1), No. 416.
(43) Zeng, Z.; Xu, J.; Zhao, Y.; Li, J.; Du, C.; Sun, Y.; Xiong, H. Tuning the Microenvironment of Co−N4 Ensemble for Co Single-Atom Catalysts for Electrocatalytic CO_2 Reduction. *ChemCatChem* **2024**, *16* (15), No. e202400091.
(44) Xiao, X.; Gao, Y.; Zhang, L.; Zhang, J.; Zhang, Q.; Li, Q.; Bao, H.; Zhou, J.; Miao, S.; Chen, N.; et al. A Promoted Charge Separation/Transfer System from Cu Single Atoms and C_3N_4 Layers for Efficient Photocatalysis. *Adv. Mater.* **2020**, *32* (33), No. 2003082.
(45) Cao, Y.; Chen, S.; Luo, Q.; Yan, H.; Lin, Y.; Liu, W.; Cao, L.; Lu, J.; Yang, J.; Yao, T.; Wei, S. Atomic-Level Insight into Optimizing the Hydrogen Evolution Pathway over a Co1-N4 Single-Site Photocatalyst. *Angew. Chem., Int. Ed.* **2017**, *56* (40), 12191−12196.
(46) Chen, Z.; Mitchell, S.; Vorobyeva, E.; Leary, R. K.; Hauert, R.; Furnival, T.; Ramasse, Q. M.; Thomas, J. M.; Midgley, P. A.; Dontsova, D.; et al. Stabilization of Single Metal Atoms on Graphitic Carbon Nitride. *Adv. Funct. Mater.* **2017**, *27* (8), No. 1605785.
(47) Yu, F.; Huo, T.; Deng, Q.; Wang, G.; Xia, Y.; Li, H.; Hou, W. Single-atom cobalt-hydroxyl modification of polymeric carbon nitride for highly enhanced photocatalytic water oxidation: ball milling increased single atom loading. *Chem. Sci.* **2022**, *13* (3), 754−762.
(48) Pan, D.; Deng, S.; Chen, L.; Tian, Z. A New Model of Carbon Nitride as a Substrate to Support Single Metal Atom. *J. Phys. Chem. C* **2024**, *128* (17), 7106−7114.
(49) Li, J.; Zhang, H.; Samarakoon, W.; Shan, W.; Cullen, D. A.; Karakalos, S.; Chen, M.; Gu, D.; More, K. L.; Wang, G.; et al. Thermally Driven Structure and Performance Evolution of Atomically Dispersed FeN_4 Sites for Oxygen Reduction. *Angew. Chem., Int. Ed.* **2019**, *58* (52), 18971−18980.
(50) Qin, X.; Zhu, S.; Xiao, F.; Zhang, L.; Shao, M. Active Sites on Heterogeneous Single-Iron-Atom Electrocatalysts in CO_2 Reduction Reaction. *ACS Energy Lett.* **2019**, *4* (7), 1778−1783.
(51) Li, Y.; Shan, W.; Zachman, M. J.; Wang, M.; Hwang, S.; Tabassum, H.; Yang, J.; Yang, X.; Karakalos, S.; Feng, Z.; Wang, G.;

https://doi.org/10.1021/acs.jpcc.4c08562
J. Phys. Chem. C 2025, 129, 7327−7334

Wu, G. Atomically Dispersed Dual-Metal Site Catalysts for Enhanced CO_2 Reduction: Mechanistic Insight into Active Site Structures. *Angew. Chem., Int. Ed.* **2022**, *61* (28), No. e202205632.
(52) Jiang, L.; Yuan, X.; Pan, Y.; Liang, J.; Zeng, G.; Wu, Z.; Wang, H. Doping of graphitic carbon nitride for photocatalysis: A reveiw. *Appl. Catal., B* **2017**, *217*, 388−406.
(53) Liu, F.; Deng, J.; Su, B.; Peng, K.-S.; Liu, K.; Lin, X.; Hung, S.-F.; Chen, X.; Lu, X. F.; Fang, Y.; et al. Poly(triazine imide) Crystals for Efficient CO_2 Photoreduction: Surface Pyridine Nitrogen Dominates the Performance. *ACS Catal.* **2025**, *15* (2), 1018−1026.
(54) Su, B.; Zheng, M.; Lin, W.; Lu, X. F.; Luan, D.; Wang, S.; Lou, X. W. S-Scheme Co_9S_8@$Cd_{0.8}Zn_{0.2}$S-DETA Hierarchical Nanocages Bearing Organic CO_2 Activators for Photocatalytic Syngas Production. *Adv. Energy Mater.* **2023**, *13* (15), No. 2203290.
(55) Kottwitz, M.; Li, Y.; Palomino, R. M.; Liu, Z.; Wang, G.; Wu, Q.; Huang, J.; Timoshenko, J.; Senanayake, S. D.; Balasubramanian, M.; et al. Local Structure and Electronic State of Atomically Dispersed Pt Supported on Nanosized CeO_2. *ACS Catal.* **2019**, *9* (9), 8738−8748.
(56) Zhang, S.; Tang, Y.; Nguyen, L.; Zhao, Y.-F.; Wu, Z.; Goh, T.-W.; Liu, J. J.; Li, Y.; Zhu, T.; Huang, W.; et al. Catalysis on Singly Dispersed Rh Atoms Anchored on an Inert Support. *ACS Catal.* **2018**, *8* (1), 110−121.
(57) Kottwitz, M.; Li, Y.; Wang, H.; Frenkel, A. I.; Nuzzo, R. G. Single Atom Catalysts: A Review of Characterization Methods. *Chemistry − Methods* **2021**, *1* (6), 278−294.
(58) Wang, X.; Chen, X.; Thomas, A.; Fu, X.; Antonietti, M. Metal-Containing Carbon Nitride Compounds: A New Functional Organic-Metal Hybrid Material. *Adv. Mater.* **2009**, *21* (16), 1609−1612.
(59) de Carvalho, N. A.; Wang, Y.; Morales-Soto, N.; Waldeck, D.; Bibby, K.; Doudrick, K.; Gilbertson, L. M. Using C-Doping to Identify Photocatalytic Properties of Graphitic Carbon Nitride That Govern Antibacterial Efficacy. *ACS ES&T Water* **2021**, *1* (2), 269−280.
(60) Zheng, D.; Pang, C.; Liu, Y.; Wang, X. Shell-engineering of hollow g-C_3N_4 nanospheres via copolymerization for photocatalytic hydrogen evolution. *Chem. Commun.* **2015**, *51* (47), 9706−9709.
(61) Che, W.; Cheng, W.; Yao, T.; Tang, F.; Liu, W.; Su, H.; Huang, Y.; Liu, Q.; Liu, J.; Hu, F.; et al. Fast Photoelectron Transfer in (C_{ring})−C_3N_4 Plane Heterostructural Nanosheets for Overall Water Splitting. *J. Am. Chem. Soc.* **2017**, *139* (8), 3021−3026.
(62) Vidyasagar, D.; Ghugal, S. G.; Umare, S. S.; Banavoth, M. Extended π-conjugative n-p type homostructural graphitic carbon nitride for photodegradation and charge-storage applications. *Sci. Rep.* **2019**, *9* (1), No. 7186.
(63) Niu, W.; Marcus, K.; Zhou, L.; Li, Z.; Shi, L.; Liang, K.; Yang, Y. Enhancing Electron Transfer and Electrocatalytic Activity on Crystalline Carbon-Conjugated g-C_3N_4. *ACS Catal.* **2018**, *8* (3), 1926−1931.
(64) Ma, L.; Fan, H.; Fu, K.; Lei, S.; Hu, Q.; Huang, H.; He, G. Protonation of Graphitic Carbon Nitride (g-C_3N_4) for an Electrostatically Self-Assembling Carbon@g-C_3N_4 Core−Shell Nanostructure toward High Hydrogen Evolution. *ACS Sustainable Chem. Eng.* **2017**, *5* (8), 7093−7103.
(65) Chuang, P.-K.; Wu, K.-H.; Yeh, T.-F.; Teng, H. Extending the π-Conjugation of g-C_3N_4 by Incorporating Aromatic Carbon for Photocatalytic H_2 Evolution from Aqueous Solution. *ACS Sustainable Chem. Eng.* **2016**, *4* (11), 5989−5997.
(66) Wang, Y.; Bai, X.; Qin, H.; Wang, F.; Li, Y.; Li, X.; Kang, S.; Zuo, Y.; Cui, L. Facile One-Step Synthesis of Hybrid Graphitic Carbon Nitride and Carbon Composites as High-Performance Catalysts for CO_2 Photocatalytic Conversion. *ACS Appl. Mater. Interfaces* **2016**, *8* (27), 17212−17219.
(67) Zhou, Y.; Zhang, L.; Huang, W.; Kong, Q.; Fan, X.; Wang, M.; Shi, J. N-doped graphitic carbon-incorporated g-C_3N_4 for remarkably enhanced photocatalytic H_2 evolution under visible light. *Carbon* **2016**, *99*, 111−117.

https://doi.org/10.1021/acs.jpcc.4c08562
J. Phys. Chem. C 2025, 129, 7327−7334